JPP Journal of Pharmacy and Pharmacology

JPP 2009, 61: 1155–1161

Received February 19, 2009
Accepted June 1, 2009
DOI 10.1211/jpp/61.09.0004
ISSN 0022-3573

Research Paper

Mannose 6-phosphate-modified bovine serum albumin nanoparticles for controlled and targeted delivery of sodium ferulate for treatment of hepatic fibrosis

Feng-Qian Li[a], Hua Su[b], Xu Chen[a], Xian-Ju Qin[a], Ji-Yong Liu[b], Quan-Gang Zhu[b] and Jin-Hong Hu[b]

[a]Shanghai Eighth People's Hospital, Shanghai, China and [b]Changhai Hospital, Second Military Medical University, Shanghai, China

Abstract

Objectives The aim was to prepare neoglycoprotein-based nanoparticles for targeted drug delivery to hepatic stellate cells, and to evaluate their characteristics *in vitro* and *in vivo*.
Methods The neoglycoprotein of bovine serum albumin modified with mannose 6-phosphate was synthesised from mannose, and used as wall material to nanoencapsulate the model natural antifibrotic substance sodium ferulate using a desolvation method. The morphology, drug loading capacity, release *in vitro* and biodistribution *in vivo* of the nanoparticles were studied. Selectivity of the nanoparticles for hepatic stellate cells was evaluated by immunohistochemical analysis of fibrotic rat liver sections.
Key findings The spherical nanoparticles were negatively charged with zeta potential ranging from −2.73 to −35.85 mV, and sizes between 100 and 200 nm with a narrow size distribution. Drug entrapment efficiency of about 90% (w/w) and loading capacity of 20% (w/w) could be achieved. *In vitro*, the nanoparticles showed an initial rapid continuous release followed by a slower sustained release. After intravenous injection into mice, the nanoparticles showed a slower elimination rate and a much higher drug concentration in liver compared with the sodium ferrate solution, and less distribution to the kidneys and other tissues. Immunohistochemistry indicated that the neoglycoprotein-based nanoparticles were taken up specifically by hepatic stellate cells.
Conclusions The nanoparticles may be an efficient drug carrier targeting hepatic stellate cells.
Keywords desolvation procedure; hepatic stellate cells specificity; liver targeting; neoglycoprotein nanoparticles; sodium ferulate

Introduction

Developments in biochemistry, immunohistochemistry and molecular biology have considerably advanced our understanding of the pathogenic mechanisms of hepatic fibrosis. The activation and proliferation of hepatic stellate cells (HSCs) contribute to the transformation of intrahepatic connective tissue into myofibroblasts, which results in increased extracellular matrix deposition and ultimately the formation of liver fibrosis.[1–3] The important role of HSCs in the progression of liver fibrosis makes these cells a potential target for therapeutic intervention. Drugs with antifibrotic activities exert their pharmacological actions either inside HSCs or at the cell membrane. However, most antifibrotic drugs do not accumulate in HSCs and hence lack effectiveness or produce unwanted side-effects outside the target cells.[4,5]

The mannose 6-phosphate (M6P)/insulin-like growth factor 2 (IGF-2) receptor is expressed on activated rat HSCs, particularly during the fibrosis process.[6] About 10–20% of receptors are expressed on the cell surface, and the receptor has specific binding sites for M6P- and IGF-2-containing ligands. Previous research has shown that human serum albumin (HSA) substituted with M6P groups binds predominantly to HSCs in rats with liver fibrosis.[7] The binding and uptake of this modified albumin by quiescent and activated HSCs was also examined. The authors concluded that M6P-HSA would be applicable as an HSC-selective carrier for intracellular delivery of antifibrotic drugs.[8]

Correspondence: Dr Feng-Qian Li, Department of Pharmaceutics, Shanghai Eighth People's Hospital, Shanghai 200235, China. E-mail: fqlijr@gmail.com

This might also have implications for the design of novel therapeutic strategies for the treatment of liver fibrosis.

In addition to the liver and HSC specificity of M6P-HSA, other features might determine the applicability of this neoglycoprotein or influence the choice of the drug to be coupled. Few reports have considered the conjugation of an antifibrotic agent to M6P-HSA, and the neoglycoprotein analogue grafted with M6P has seldom been used as an encapsulation material for drug entrapment studies.

Sodium ferulate (SF; 3-methoxy-4-hydroxy-cinnamate), a salt of ferulic acid, is a natural substance used in traditional Chinese medicine for the treatment of cardiovascular and cerebrovascular diseases and to prevent thrombosis.[9] SF has been shown to be a potential candidate for the treatment of hepatic fibrosis.[10,11] Recently, we prepared SF-entrapping bovine serum albumin (BSA) nanoparticles and demonstrated passive liver-targeted delivery.[12] Nanoencapsulation of SF into M6P-modified BSA may therefore provide HSC-specific drug delivery.

In the current work, BSA was modified with M6P (synthesised from mannose) and used as the wall material to encapsulate SF using a desolvation procedure. The obtained neoglycoprotein SF-M6P-BSA nanoparticles were characterised in terms of morphology, drug loading capacity (LC), release *in vitro* and biodistribution *in vivo*. Immunohistochemistry was performed on fibrotic rat liver sections to evaluate the potential HSC-specific selectivity of the SF-M6P-BSA nanoparticles.

Materials and Methods

Reagents and animals

BSA was purchased from Sino-American Biotechnology Co. (Shanghai, China), D-mannose was from Shanghai Fengsun Fine Chemical Limited Company (Shanghai, China), Sephadex G-50 gel from Pharmacia (Shanghai, China), Dowex ion-exchange resin $50X_2$ from J&K China Chemical Limited Company (Beijing, China) and SF from Limin Pharmaceutical Factory of Lizhu Group (Shaoguan, China). Ethanol and glutaraldehyde (25% v/v) were obtained from the Chemical Agent Station, Medicine Group of China (Shanghai, China). HPLC-grade methanol and acetic acid were from Sigma-Aldrich (Steinheim, Germany). All other chemicals were of analytical grade.

Kunming mice (20 ± 2 g) and Sprague-Dawley rats (250 ± 10 g) were supplied by the experimental animal centre of the Second Military Medical University (Shanghai, China). All procedures were approved by the Animal Care and Supply Committee of the Second Military Medical University.

Synthesis and purification of neoglycoprotein M6P-BSA

BSA was modified with M6P according to the methods of Beljaars and colleagues[7] and Zhang and colleagues.[13] The starting material, D-mannose, was acetylated, isomerised, conjugated with *p*-nitrophenol and then deacetylated. The *p*-nitrophenyl-α-D-mannopyranoside pivotal intermediate obtained was phosphorylated and the nitro group was subsequently reduced with 10% palladium on active carbon. The *p*-aminophenyl-6-phospho-α-D-mannopyranoside produced was coupled to BSA activated by thiophosgene. The coupling degree of M6P was determined by the phenol–sulfuric acid method,[14] and the BSA content was determined using the bicinchoninic acid (BCA) protein assay.[15]

Table 1 Sugar densities detected in neoglycoproteins synthesised with different ratios of bovine serum albumin to mannose 6-phosphate

Compound	BSA (μmol)	M6P (mmol)	Sugar : BSA ratio in product (mol/mol, n = 3)
1	0.23	0.04	1.0 ± 0.07
2	0.23	0.07	1.7 ± 0.12
3	0.23	0.09	2.6 ± 0.18
4	2.30	0.45	3.75 ± 1.37
5	1.10	0.50	6.23 ± 0.30
6	1.10	0.90	10.26 ± 1.05

BSA, bovine serum albumin; M6P, mannose-6-phosphate.

Neoglycoproteins with different degrees of substitution were synthesised by varying the molar ratio of BSA and *p*-aminophenyl-6-phospho-α-D-mannopyranoside (Table 1).

The obtained sugar conjugate was dialysed against 0.15 mol/l NaCl (2 × 500 ml) and distilled water (4 × 500 ml) then lyophilised to white powder. The crude product was purified initially by Sephadex G-50 gel chromatography and then using Dowex-$50X_2$ ion-exchange resin, eluting with 0.15 mol/l NaCl and distilled water, respectively. The products were stored at −20°C until use.

Preparation of SF-loaded neoglycoprotein nanoparticles

The neoglycoprotein nanoparticles were prepared using a previously reported desolvation method.[12,16,17] M6P-BSA and SF were dissolved in phosphate-buffered saline (PBS) and the pH of the aqueous mixture adjusted to about 6.0. With the addition of 95% ethanol (7–9 ml added at constant rate), the albumin solution spontaneously transformed into an opalescent suspension and the nanoparticles emerged under continuous magnetic stirring (500 rpm) at room temperature. After the desolvation procedure, glutaraldehyde solution (8% v/v) was added very slowly with continuous stirring over 24 h to induce cross-linkage of the desolvated nanoparticles. Details of the ethanol (desolvation agent) addition rate and other formation conditions (amounts of M6P-BSA, SF, glutaraldehyde) are given in Table 2.

Ethanol in the prepared colloidal sample was eliminated by evaporation under reduced pressure (0.08 MPa, 50 rpm) at room temperature. The resulting nanoparticles were then purified and obtained by centrifugation at 20 000*g* at 15°C for 30 min. After 12 h of prefreezing at −20°C, the lyophilisation step was finally performed for 24 h with 5% lactose (w/v) as the cryoprotector.

Morphology, size and zeta potential of SF-loaded neoglycoprotein nanoparticles

After negative staining, the morphology of the prepared neoglycoprotein nanoparticles was examined using an H-600 transmission electron microscope (TEM; Hitachi, Japan). The size and charge of the nanoparticles were analysed by electrophoretic light scattering using a Nicomp 380 ZLS

Table 2 Effect of formulation parameters on characteristics of sodium ferulate-mannose-6-phosphate-bovine serum albumin nanoparticles

SF (mg)	M6P-BSA (mg)	Glutaraldehyde (μl)	Ethanol addition rate (ml/min)	Mean size (nm)	Zeta potential (–mV)	Loading capacity (%)	Encapsulation efficiency (%)
3	20	5	0.6	135.3 ± 15.07	–26.41 ± 3.57	1.92 ± 1.07	13.07 ± 7.47
5	**20**	**5**	**0.6**	**151.9 ± 31.13**	**–30.17 ± 1.38**	**12.33 ± 0.44**	**56.26 ± 2.31**
7	20	5	0.6	187.8 ± 25.50	–35.85 ± 3.89	20.10 ± 2.29	71.87 ± 10.23
10	20	5	0.6	214.3 ± 21.13	–21.13 ± 2.20	14.48 ± 5.58	33.87 ± 14.66
5	10	5	0.6	187.3 ± 25.60	–2.73 ± 3.65	21.72 ± 1.52	55.56 ± 5.01
5	40	5	0.6	207.6 ± 15.76	–24.53 ± 2.56	8.17 ± 0.32	71.17 ± 3.07
5	50	5	0.6	262.8 ± 35.88	–24.55 ± 1.68	7.80 ± 0.15	84.56 ± 1.76
5	20	10	0.6	172.5 ± 26.17	–25.88 ± 1.03	18.25 ± 0.33	91.01 ± 2.17
5	20	15	0.6	163.2 ± 21.80	–26.89 ± 2.23	16.00 ± 0.59	77.65 ± 3.57
5	20	20	0.6	122.7 ± 24.48	–32.39 ± 2.06	8.82 ± 1.01	36.94 ± 7.68
5	20	5	0.3	103.0 ± 24.27	–18.04 ± 1.94	12.99 ± 0.88	59.74 ± 4.65
5	20	5	0.9	208.2 ± 18.46	–21.36 ± 2.75	15.86 ± 0.56	75.40 ± 3.15
5	20	5	1.2	217.3 ± 25.13	–13.59 ± 1.59	13.73 ± 1.44	63.76 ± 7.69

Values are means ± SD (n = 3). The nanoparticles used for in-vitro and in-vivo studies are shown in bold. BSA, bovine serum albumin; M6P, mannose-6-phosphate; SF, sodium ferulate.

Coulter (Santa Barbara, CA, USA). The measurements were performed in triplicate at a temperature of 25°C.

Drug loading capacity and encapsulation efficiency of nanoparticles

Drug encapsulation efficiency (EE) and LC of the prepared SF-M6P-BSA nanoparticles were determined using the methods we have described previously.[12] The SF concentration in the supernatant obtained after ultracentrifugation of nanoparticle colloidal samples was determined by HPLC. The amount of SF entrapped in the nanoparticles was calculated by the difference between the amount of SF initially added and the free SF recovered in the supernatant. Each sample was assayed in triplicate.

In-vitro release of SF from the nanoparticles

The in-vitro release of SF from SF-M6P-BSA nanoparticles was determined as follows. About 30 mg of the lyophilised nanoparticles was placed into a dialysis membrane bag with a molecular cut-off of 8 kDa, which was tied and placed in 100 ml PBS (pH 7.4). The entire release system was incubated at 37°C under stirring (50 rpm). At scheduled time intervals, a sample of the release medium (0.5 ml) was removed and replaced with the same volume of fresh PBS. The amount of SF in the release medium was determined by HPLC.[12] The cumulative percentage of SF released was then plotted versus time. All measurements were performed in triplicate.

Tissue distribution

We have previously studied the biodistribution of SF-loaded BSA nanoparticles *in vivo*.[12] We used the same method in the present study to determine the distribution of SF-M6P-BSA nanoparticles and SF solution in mice. SF-M6P-BSA nanoparticles were injected intravenously into mice via the lateral tail vein (1.0 mg SF/kg). Blood samples (about 1 ml) were taken at 0.25, 0.5, 1, 2, 3, 4, 6, 8, 10, 12 and 24 h after administration. At the final 24 h time point the animals were killed by cervical dislocation and the heart, liver, spleen, lungs and kidney were excised, dried with filter paper, weighed and then homogenised prior to analysis. Levels of SF in blood and tissue samples were determined using reverse-phase HPLC, using tinidazole as the internal standard.[18]

Liver immunohistochemistry

Male Sprague-Dawley rats were housed under standard laboratory conditions with free access to food and water. Liver fibrosis was induced by bile duct ligation (BDL) performed under general anaesthesia induced with 3% (w/v) pentobarbital (30 mg/kg i.p.). The 3 weeks following BDL is characterised by excessive matrix deposition and activation of HSCs.[19] Rats were used for immunohistochemistry 3 weeks after BDL.

Normal and BDL rats were fasted overnight before experiments, and the BDL rats were divided randomly into control and test groups. The BDL test rats were given SF-M6P-BSA nanoparticles (10 mg SF/kg) injected via the tail vein; the BDL control group and normal rats were injected with saline. Twenty minutes after drug administration, by which time nanoparticles would have distributed to liver and been delivered to HSCs, rats were killed by cervical dislocation and samples of liver were prepared and fixed in 10% (v/v) neutral buffered formaldehyde solution, then processed for immunohistochemical analysis. Paraffin wax sections (4 μm) of the liver were stained for the presence of M6P-modified albumin nanoparticles with a rabbit polyclonal antibody directed against BSA (Dako, Glostrup, Denmark) using a standard indirect immunoperoxidase method.[20]

Portal and central HSCs in fibrotic rat livers were identified using double-immunostaining using mouse monoclonal primary anti-desmin and anti-glial fibrillary acidic protein (GFAP) antibodies (Santa Cruz Biotechnology, Santa Cruz, CA, USA).[21] To assess whether the modified albumin nanoparticles were taken up specifically by HSC, we stained consecutive liver sections and photographed them at the same magnification for comparison.

Statistical analysis

Data are presented as means ± SD. Results of the in-vivo biodistribution studies were analysed using the Kruskal–Wallis test. Differences were considered to be significant at $P < 0.05$.

Results

Synthesis of M6P-BSA

Early reports[7] showed the successful modification of HSA with M6P, which selectively delivered antifibrotic drugs to HSCs. The coupling of M6P to albumin yielded a water-soluble neoglycoprotein. In this work, we prepared different sugar-contained neoglycoproteins by varying the molar ratio of M6P to BSA during the grafting process (Table 1). As shown in Table 1, a series of M6P-BSA was obtained in which the number of M6P molecules per BSA molecule ranged from 1.0 to 10.26. The sugar density linked to BSA increased with increasing M6P content.

Desolvation process and characterisation of nanoparticles *in vitro*

A controlled desolvation procedure[22,23] was used to prepare the colloidal system of the neoglycoprotein nanoparticles with well-defined physicochemical characteristics. With addition of ethanol, M6P-BSA was phase separated from the solution as its water solubility diminished. Nanoparticles were then formed from the M6P-BSA solution with desolvation achieved by the addition of ethanol. Almost all the M6P-BSA carrier material used was involved in nanoencapsulation, and a particle yield over 92% could be obtained (measured by the BCA protein assay).[12]

Typical TEM images of the M6P-modified nanoparticles and their morphology characteristics are shown in Figure 1. The SF-loaded neoglycoprotein nanoparticles (Figure 1b) had an irregular spherical shape with a relatively narrow size distribution, whereas the blank M6P-BSA nanoparticles (Figure 1a) were more spherical and smoother. It thus appears that the embedded drug might be irregularly located within the M6P-anchored BSA nanoparticles, seemingly shaped with the 'core-shell' structure.

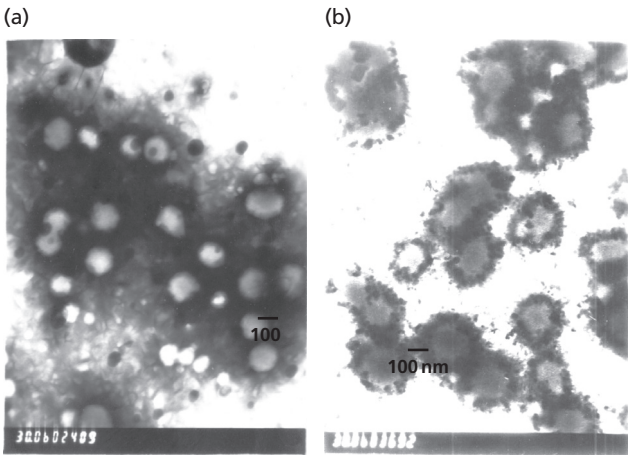

Figure 1 Transmission electron micrographs of mannose-6-phosphate modified nanoparticles. The images (×30 000) show (a) M6P-BSA nanoparticles and (b) SF-M6P-BSA nanoparticles prepared by the desolvation method (pH 6, 20 mg M6P-BSA, 5 mg, SF, 5 μl glutaraldehyde (8% v/v), ethanol addition rate of 0.6 ml/min). BSA, bovine serum albumin; M6P, mannose-6-phosphate; SF, sodium ferulate.

During the initial desolvation of M6P-BSA, the size of the formed nanoparticles decreased (Table 2). As the M6P-BSA added increased up to about 50 mg, the particle size of nanoparticles increased to 262.8 nm as a result of polymerisation (Table 2). As shown in Table 2, there was an obvious size decrease to 122.7 nm in particles cross-linked with increasing amounts of glutaraldehyde (20 μl, 8% v/v), reflecting the influence of the cross-linker on the particle diameter. The ethanol addition rate (0.3–1.2 ml/min) had a significant influence on the mean diameter of the neoglycoprotein nanoparticles produced, which increased steadily from 103 to 217.3 nm (Table 2).

Table 2 also shows the influence of the formulation parameters on the zeta potential of the albumin nanoparticles. Almost all measurements of zeta potential were between −30 and −20 mV (Table 2), far lower than the zeta potential of −2.73 mV for nanoparticles prepared with the lowest concentration of M6P-BSA (10 mg dissolved in 3 ml). This phenomenon may be related to the negative charges of M6P groups in the modified BSA.

Usually, the expected drug content reflects the LC in nanoencapsulation. EE is calculated by relating the actual drug content to the amount of drug added. As shown in Table 2, EE increased as the amount of M6P-BSA added was increased. More desolvated M6P-BSA might increase the encapsulation of SF dissolved in the internal aqueous phase. The EE of SF increased from 55.56% to 84.56% as the amount of M6P-BSA increased from 10 mg to 50 mg, whereas LC decreased from 21.72% to 7.8% (Table 2). The rapid decrease in LC might be because nanoparticles formed quickly under these conditions and so entrapped less drug. Table 2 shows that LC and EE increased as the drug concentration was increased from 3.0 to 7.0 mg (LC from 1.92% to 20.10% and EE from 13.07% to 71.87%) but declined when the amount of SF exceeded 10 mg.

As the amount of cross-linker increased from 10 to 20 μl, EE decreased dramatically from 91.01% to 36.94%, and LC from 18.25% to 8.82%. Although affected by the addition rate of ethanol (0.3–1.2 ml/min), EE and LC were relatively constant (Table 2). The ethanol addition rate of 0.9 ml/min resulted in a dramatic increase in EE to 75.4% and LC to 15.86%, indicating that the ethanol addition rate must be slow and controlled below 0.9 ml/min.

In-vitro release studies

The drug release profiles obtained *in vitro* show the cumulative release of SF from SF-M6P-BSA nanoparticles relative to the amount of SF encapsulated. As shown in Figure 2, there was a rapid continuous and constant release of SF from the nanoparticles, presumably due to the diffusion of the drug from the particle surface. The amount of released SF increased slightly from 2.5 to about 5 h, but then remained constant to 12 h, implying that drug release is finished by about 5 h, and that in fact most of it is released in the first 2.5 h. The cumulative drug release in 12 h reached 85.94% (Figure 2), which may include the drug embedded within the interior of the albumin matrix.[24] A significant amount of SF loaded in the external surface of the nanoparticle might account for the initial burst release of SF (1–2.5 h) whereas the subsequent drug release during the plateau state seemed to be due to the SF entrapped within the nanoparticles.

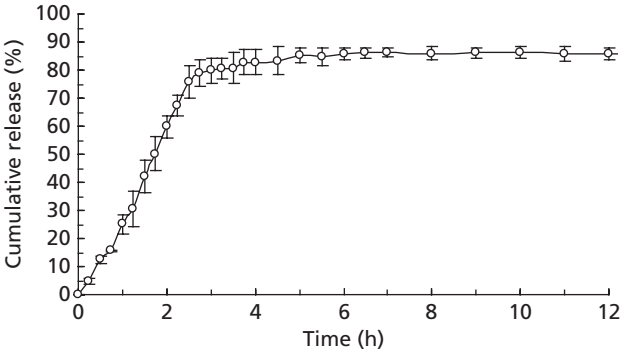

Figure 2 Drug-release profile from mannose-6-phosphate modified nonoparticles. In-vitro release profile of sodium ferulate (SF) from SF-M6P-BSA nanoparticles in phophate-buffered saline (pH 7.4). Formulation conditions for nanoparticles are described in Figure 1. Data are means ± SD ($n = 3$). BSA, bovine serum albumin; M6P, mannose-6-phosphate.

In-vivo distribution of nanoparticles

We have previously reported liver targeting of SF-nanoencapsulating BSA (SF-BSA) nanoparticles.[12] Figure 3 shows that in the liver in the present biodistribution experiments the drug concentration in the livers of mice increased quickly to 0.5 h and then decreased steeply.

Compared with SF solution, both SF-BSA and SF-M6P-BSA nanoparticles showed high hepatic drug levels at almost all time points. Drug concentrations during the first 4 h in the rats given SF-loaded nanoparticles were 2–4 times higher than in those given SF solution; the drug concentration with the SF solution group was much lower 8 h after administration (< 0.09 μg/g). Furthermore, the concentration of SF in the livers of the two nanoparticle-treated groups at 6, 8 and 12 h were over 10-fold those in the SF solution group (Figure 3). The drug concentration profiles were similar in the two nanoparticle groups.

The amount of drug distributed to various tissues after intravenous injection was calculated from the SF concentration and organ weight, and the drug distribution percentage (DDP) for each organ (blood, heart, liver, spleen, lungs and kidneys) determined as the proportion of the total drug amount that had accumulated in that organ. Figure 4 shows the DDPs in tissues of mice after intravenous administration of SF solution and SF-M6P-BSA nanoparticles from 0.25 to 12 h. As shown in Figure 4a, after injection with SF solution, drug was principally distributed to the liver and kidneys. After 4 hours, hepatic drug accumulation decreased from 86.38% (4 h) to 30.43% (12 h), whilst the DDP increased largely in the kidneys – to 69.56% (12 h), illustrating the main excretion pathway for intravenously injected SF and its possible toxicity to kidneys. In the mice dosed with nanoparticles, the DDP in kidney remained below 30% (Figure 4b); 12 h after the injection, the DDP in kidney had decreased steeply to 17.92%, which is almost 4 times less than that for the SF solution (Figure 4a). This change in the drug distribution property profile may be helpful in decreasing the unwanted effects of SF on the kidneys. DDP in the livers of mice injected with SF-M6P-BSA nanoparticles remained above 80% for 2 to 12 h after administration (Figure 4b), which presumably reflects sustained release of drug from the nanoparticles.

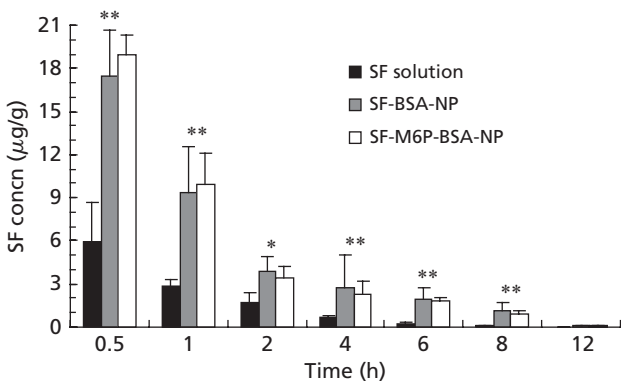

Figure 3 In-vivo accumulation of nonoparticles in liver. Liver concentrations of sodium ferulate (SF) following intravenous injection of SF solution, SF-BSA-NP or SF-M6P-BSA-NP to mice. Formulation conditions for nanoparticles are described in Figure 1. Data are means ± SD ($n = 3$). *$P < 0.05$, **$P < 0.01$ vs SF solution. BSA, bovine serum albumin; M6P, mannose-6-phosphate; NP, nanoparticles.

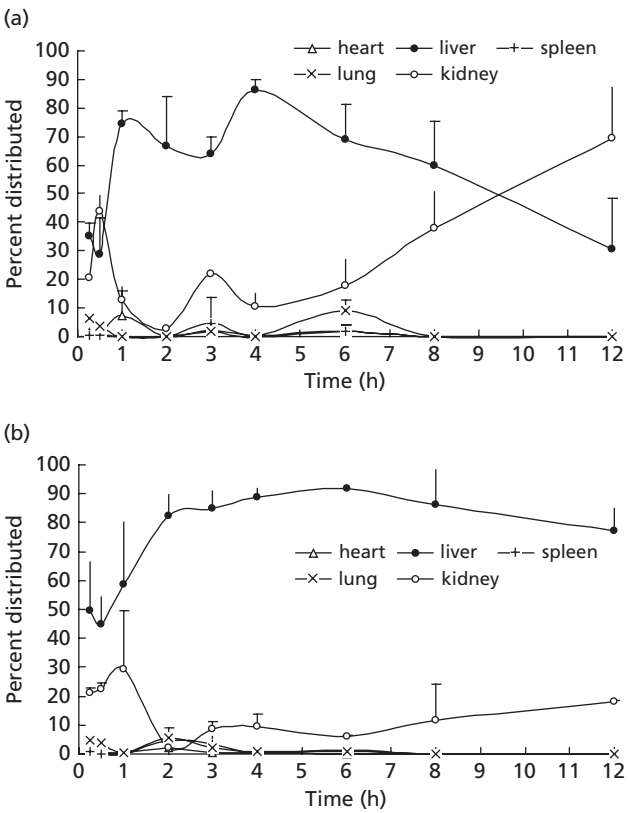

Figure 4 In-vivo distribution of nanoparticles in various tissues. Distribution of sodium ferulate (SF) in mice following intravenous injection of (a) SF solution or (b) SF-M6P-BSA nanoparticles (prepared using the conditions detailed in Figure 1). Data are means ± SD ($n = 3$). The differences between the two formulations are significant for heart and lung ($P < 0.05$), liver and kidney ($P < 0.01$). BSA, bovine serum albumin; M6P, mannose-6-phosphate.

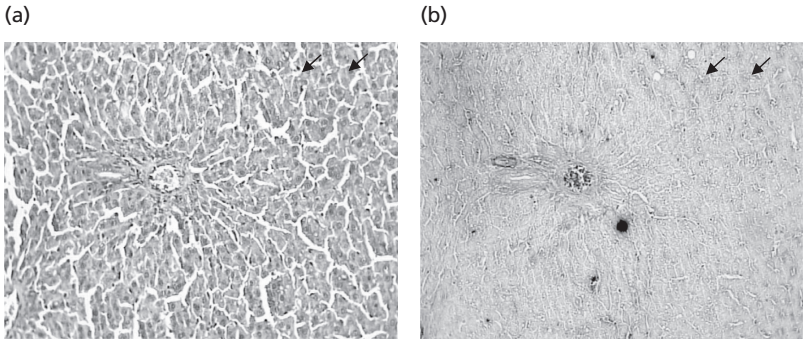

Figure 5 Immunohistochemical analysis of the uptake by hepatic stellate cells in fibrotic livers. Two consecutive liver sections were stained and photographed at the same magnification for comparison. Positive stains are indicated with arrows. Original magnification ×200. (a) Stained to identify M6P-BSA nanoparticles with a polyclonal antibody direct against human serum albumin; (b) double staining of hepatic stellate cells (HSC) with anti-desmin and anti-GFAP antibodies. BSA, bovine serum albumin; M6P, mannose-6-phosphate.

Immunohistochemical detection of SF-M6P-BSA nanoparticles *in vivo*

Figure 5 shows two consecutive liver sections from rats with fibrosis, photographed at the same magnification, showing positively stained M6P-BSA nanoparticles (Figure 5a) and positively stained HSCs in the corresponding spots (Figure 5b). However, hepatic cells also stained positively, making it difficult to discount the possibility of albumin secretion from hepatic cells themselves. In their early work, Beljaars and colleagues[8] incubated slices of liver with ^{125}I-M6P$_{28}$-HSA and ^{125}I-HSA for immunohistochemical test in order to demonstrate whether HSC binding was via M6P$_{28}$-HSA or HSA. The albumin was detected with polyclonal anti-HSA antibodies and the results noted positively stained HSCs in M6P$_{28}$-HSA group but the absence of staining in the HSA group. These findings also indicate that HSCs do not secrete albumin themselves. Thus, we are confident that our results show specific binding of the prepared M6P-BSA nanoparticles to HSCs, and the positive staining in Figure 5 probably reflects the active absorption of M6P-BSA nanoparticles by HSCs.

Discussion

BSA is often used as a natural material for drug encapsulation because of its biocompatibility and biodegradability. Beljaars and colleagues have previously shown that the more M6P groups coupled to albumin, the higher the net negative zeta potential of the neoglycoprotein.[7] The negatively charged neoglycoprotein was useful for SF encapsulation and further hepatic targeting *in vivo*.[12] The derivative of M6P$_{10}$-BSA synthesised with 1.1 μmol BSA and 0.9 mmol M6P (as indicated in Table 1) was selected as wall material and used for subsequent in-vitro and in-vivo experiments. As for the SF-loaded neoglycoprotein nanoparticles formed after the desolvation process, re-solubilsation in aqueous medium is possible. Following the ethanol desolvation, it is necessary to stabilise the albumin wall material. In this work, further cross-linking with glutaraldehyde was carried out to solidify the desolvated SF-M6P-BSA nanoparticles and to control the drug release rate.

Repulsion forces between the negatively charged particles might contribute to the initially decreased particle size. Then the increased mean particle size was considered to be formed by the enriched M6P-BSA wall material. This is similar to the previous results which showed the influence of the amount of wall material on particle diameter.[16] For the more closely constructed neoglycoprotein nanoparticles (involving the lysine side chains of protein), reduction in diameter could be expected with the enhanced degree of cross-linking. The quick desolvation process might also lead to large aggregates of nanoparticles or even precipitation (Table 2). The puff-structured nanoparticles formed with relatively large diameter might reflect the fast albumin-phase transformation rate at higher ethanol flow rates. The difference in drug concentration between the internal and external aqueous phases could be responsible for the increased EE. The increasing drug amount promoted encapsulation into the cross-linked M6P-BSA. However, too much drug might lead to high ionic strength in the outer medium, resulting in large aggregates. Enhanced stabilisation could diminish the absorbed drug in the outer sphere of nanoparticles, thus lowering EE and LC. This is supported by the characteristics of nanoparticles cross-linked with different amount of glutaraldehyde, shown in Table 2.

The external/internal ratio of SF encapsulated could not be controlled during the nanoencapsulation process, and the amount of glutaraldehyde used as cross-linker might be important to retard drug release from albumin particles.[12] The erosion and degradation of neoglycoprotein M6P-BSA is also involved in the drug diffusion through the polymer wall during the release process.[25] In view of the biodegradability and internalisation processes of M6P-BSA nanoparticles *in vivo*, low amounts of glutaraldehyde should be used in the cross-linking stage as far as possible. The prepared SF-M6P-BSA nanoparticles were stabilised with 0.8 μl glutaraldehyde (8% v/v) per mg M6P-BSA.

The similar hepatic SF levels obtained from BSA nanoparticles and M6P-BSA nanoparticles entrapped with the same dose of SF resulted mainly from the passive targeted drug delivery of the nanoparticles, reflecting their similar particle diameter and zeta potentials. The percentage of drug in the liver was much higher than in other organs, including the kidney, further demonstrating effective liver targeting of the SF-M6P-BSA nanoparticles. The hepatic

accumulation indicated liver targeting characteristic of intravenously injected nanoparticles, which could provide the necessary precondition for further HSC-sited drug delivery. As for M6P-BSA nanoparticles, the amount of SF in the liver will include the drug distributed to hepatic tissue and that delivered into HSCs. Thus, this liver targeting does not distinguish secondary HSC targeting. The advantages of M6P-BSA nanoparticles over the mannose derivative of albumin would be indicated by immunohistochemistry studies.

From these preliminary immunohistochemical experiments, we temporarily conclude that the neoglycoprotein-based nanoparticles are specifically taken up by HSCs. The results provide useful experience for the further authentication of SF-M6P-BSA nanoparticles designed as dual targeting carriers to the liver in general and the HSCs in particular. However, it was not clear whether the nanoparticles are actual in the cells or bound to surface receptors. The actually behaviour and mechanism involved are to be studied in further cell-related work.

Conclusions

The synthesised biodegradable copolymer of neoglycoproteins (M6P-BSA) was used as wall material to successfully nanoencapsulate water-soluble SF by a desolvation method. Particle diameter, zeta potential, LC and EE of the prepared nanoparticles could be adjusted by optimising the process parameters such as amounts of M6P-BSA and SF, the concentration of glutaraldehyde and the ethanol addition rate. The in-vitro drug release profile of SF-M6P-BSA nanoparticles showed an initial continuous burst release followed by a further constant sustained release. Biodistribution studies *in vivo* showed that drug accumulated in the livers of mice given SF-M6P-BSA nanoparticles intravenously. Primary immunohistochemical analysis also illustrated the selective binding of SF-M6P-BSA nanoparticles to HSCs. Thus, these nanoparticles could serve as a suitable liver-targeted, and potential HSC-specific, drug carrier based on passive and active targeting mechanisms.

Declarations

Conflict of interest

The Author(s) declare(s) that they have no conflicts of interest to disclose.

Funding

This work was supported by the National Natural Science Foundation of China (Project 30371701, 30500639) and the emphasized fundamental investigation project of Shanghai (08JC1406900).

References

1. Alcolado R *et al*. Pathogenesis of liver fibrosis. *Clin Sci* 1997; 92: 103–112.
2. Hautekeete ML, Geerts A. The hepatic stellate (ito) cell: its role in human liver disease. *Virchows Arch* 1997; 430: 195–207.
3. Gressner AM. The cell biology of liver fibrogenesis – an imbalance of proliferation, growth arrest and apoptosis of myofibroblasts. *Cell Tissue Res* 1998; 292: 447–452.
4. Wu J, Danielsson A. Inhibition of hepatic fibrogenesis: a review of pharmacologic candidates. *Scand J Gastroenterol* 1994; 29: 385–391.
5. Schuppan D *et al*. Hepatic fibrosis – therapeutic strategies. *Digestion* 1998; 59: 385–390.
6. De Bleser PJ *et al*. Insulin-like growth factor II/mannose 6-phosphate-receptor expression in liver and serum during acute CCl_4 intoxication in the rat. *Hepatology* 1996; 23: 1530–1537.
7. Beljaars L *et al*. Albumin modified with mannose 6-phosphate: a potential carrier for selective delivery of antifibrotic drugs to rat and human hepatic stellate cells. *Hepatology* 1999; 29: 1486–1493.
8. Beljaars L *et al*. Characeristics of the hepatic stellate cell-selective carrier mannose 6-phosphate modified albumin ($M6P_{28}$-HSA). *Liver* 2001; 21: 320–328.
9. Barone E *et al*. Ferulic acid and its therapeutic potential as a hormetin for age-related diseases. *Biogerontology* 2009; 10: 97–108.
10. Wang H *et al*. Antagonizing effect of sodium ferulate on the changes of hepatic antioxidative function induced by ethanol in mice. *Acta Pharm Sin* 1997; 32: 511–514.
11. Huang J *et al*. Mechanisms of sodium ferulate inhibition of collagen synthesis in hepatic stellate cells. *Acta Pharm Sin* 2004; 39: 577–580.
12. Li FQ *et al*. Preparation and characterization of sodium ferulate entrapped bovine serum albumin nanoparticles for liver targeting. *Int J Pharm* 2008; 349: 274–282.
13. Zhang J *et al*. Synthesis of a targeting drug for antifibrosis of liver; a conjugate for delivering glycyrrhetin to hepatic stellate cells. *Glycoconjugate J* 2002; 19: 423–429.
14. Dubois M *et al*. Colorimetric method for determination of sugars and related substances. *Anal Chem* 1956; 28: 350–356.
15. Smith PK *et al*. Measurement of protein using bicinchoninic acid. *Anal Biochem* 1985; 150: 76–85.
16. Langer K *et al*. Optimization of the preparation process for human serum albumin (HSA) nanoparticles. *Int J Pharm* 2003; 257: 169–180.
17. Wartlick H *et al*. Tumour cell delivery of antisense oligonucleotides by human serum albumin nanoparticles. *J Control Release* 2004; 96: 483–495.
18. Li FQ *et al*. Development of a gradient reversed-phase HPLC method for the determination of sodium ferulate in beagle dog plasma. *J Chromatogr B* 2007; 846: 319–322.
19. Kountouras J *et al*. Prolonged bile duct obstruction: a new experimental model for cirrhosis in the rat. *Br J Exp Pathol* 1984; 65: 305–311.
20. Harms G *et al*. Glycosyl receptors in macrophage subpopulations of rat spleen and lymph node. A comparative study using neoglycoproteins and monoclonal antibodies ED1, ED2 and ED3. *Cell Tissue Res* 1990; 262: 35–40.
21. Harms G *et al*. Double immunohistochemical demonstration of antigen expressing and DNA-incorporated 5-bromodeoxyuridine in frozen and plastic embedded sections. *Acta Histochem* 1988; 36S: 353–359.
22. Lochmann D *et al*. Albumin–protamine–oligonucleotide nanoparticles as a new antisense delivery system. Part 1: Physicochemical characterization. *Eur J Pharm Biopharm* 2005; 59: 419–429.
23. Roser M *et al*. Surface-modified biodegradable albumin nano- and microspheres. II: effect of surface charges on in vitro phagocytosis and biodistribution in rats. *Eur J Pharm Biopharm* 1998; 46: 255–263.
24. Lin W *et al*. Preparation and characterisation of rose Bengal-loaded surface-modified albumin nanoparticles. *J Control Release* 2001; 71: 117–126.
25. Bilati U *et al*. Strategic approaches for overcoming peptide and protein instability within biodegradable nano- and microparticles. *Eur J Pharm Biopharm* 2005; 59: 375–388.